Fluorine Substitution Effects on the Alkyl Coupling Reaction on a Ag(111) Surface

Anumita Paul[†] and Andrew J. Gellman*

Contribution from the Department of Chemical Engineering, Carnegie Mellon University, Pittsburgh, Pennsylvania 15213

Received August 31, 1994[⊗]

Abstract: We have investigated fluorine substitution effects on the rate of coupling of adsorbed alkyl groups on a Ag(111) surface. Alkyl groups are formed by thermal dissociation of the C−I bond in adsorbed alkyl iodides. Variable heating rate temperature programmed reaction (TPR) studies were used to determine the kinetic parameters for the coupling of ethyl groups and propyl groups. They are $E_a = 15.1 \pm 0.6$ kcal/mol, $\nu = 10^{16.7\pm0.8}$ s^{-1} and $E_a = 16.9 \pm 0.4$ kcal/mol, $\nu = 10^{17.1\pm0.4}$ s^{-1}, respectively. Substitution of fluorine for hydrogen in the adsorbed alkyl groups systematically raises the coupling reaction temperature. For example, trifluoropropyl groups self-couple at temperatures ~70 K higher than propyl groups on Ag(111). Coadsorbed propyl and trifluoropropyl groups cross-couple at temperatures ~10 K higher than the propyl self-coupling reaction. The kinetic parameters evaluated from the results of this study and from results of earlier studies by X.-L. Zhou, J. M. White, and co-workers [*Surf. Sci.* **1989**, *219*, 294; *Catal. Lett.* **1989**, *2*, 375; *J. Phys. Chem.* **1991**, *95*, 5575] are used to plot linear free energy relationships (LFER) which provide insight into the electronic nature of the reaction center. The implication of the LFER plots for the surface alkyl coupling reaction is that the reaction center in the transition state is electron deficient with respect to the initial state.

1. Introduction

Despite their widespread roles as chain-propagating and chain-terminating steps in catalytically important reactions such as the Fischer−Tropsch synthesis,[1] Zeigler−Natta polymerization,[2] reactions involving thermal degradation of organometallic compounds,[3] and chemical vapor deposition processes,[4] carbon−carbon bond formation reactions remained poorly understood until very recently. Recent ultra-high-vacuum (UHV) studies on copper,[5−7] silver,[8−10] gold,[11,12] nickel,[13] and platinum[14] surfaces have addressed some of the factors such as structural effects, bond strengths, nature of the metal, coverage of the reactants, etc. controlling the rate and selectivity of the carbon−carbon bond formation reactions. However, studies which address the electronic structure of the reaction center are still lacking. This paper bridges this gap by using fluorine substitution effects as a direct means of probing the electronic nature of the reaction center during the formation of carbon−carbon bonds in the coupling reactions of adsorbed alkyl groups on the Ag(111) surface.

The basis of the fluorine substitution effect studies is as follows. Within the framework of transition state theory (TST), the rate of an elementary chemical reaction depends on the relative energies of the transition state and the initial state, i.e. on the reaction activation barrier, E_a.[15] One of the factors which contributes to the reaction barrier is the relative electron distribution in these two states. Thus if a reaction involves an initial state and a transition state which have similar electron distributions at the reaction center, the effect of an electron withdrawing (or donating) group on the energy of both the initial state and the transition state will be similar and the reaction rate will be unperturbed by substitution of this group. On the other hand, if the transition state involves an electronic structure different from that of the initial state, then an electron withdrawing substituent group will stabilize the electron rich state compared to the electron deficient state, thereby altering the reaction energetics. This basic principle has been exploited extensively in the form of linear free energy relationship (LFER) studies used in physical organic chemistry to reveal the nature of reaction centers and to elucidate reaction mechanisms in a wide variety of solution-phase and gas-phase reactions.[16−22] The LFER approach is also used to probe the reaction center in equilibrium reactions where the substituent group perturbs the initial and the final states thereby altering the equilibrium

* Author to whom all correspondence should be addressed.
[†] Present address: Molecular Physics Laboratory, SRI International, 333 Ravenswood Avenue, Menlo Park, CA 94025.
[⊗] Abstract published in *Advance ACS Abstracts*, August 15, 1995.

(1) Anderson, R. B. *The Fischer-Tropsch Synthesis*; Academic Press: New York, 1984.
(2) Boor, J. *Zeigler-Natta Catalysis and Polymerization*, 3rd ed.; Academic Press: New York, 1979.
(3) Kochi, J. K. *Organometallic Mechanism and Catalysis*; Academic Press: New York, 1978.
(4) Paul, A.; Bent, B. E. *J. Am. Chem. Soc.* Submitted for publication.
(5) Lin, J.-L.; Bent, B. E. *J. Vac. Sci. Technol. A* **1992**, *10*, 2202.
(6) Chiang, C.-M.; Wentzlaff. T. H.; Bent, B. E. *J. Vac. Sci. Technol. A* **1992**, *10*, 2185.
(7) Lin, J.-L.; Chiang, C.-M.; Jenks, C. J.; Yang, M. X.; Wentzlaff, T. H.; Bent, B. E. *J. Catal.* **1994**, *147*, 250.
(8) Zhou, X.-L.; Solymosi, F.; Blass, P. M.; Cannon, K. C.; White, J. M. *Surf. Sci.* **1989**, *219*, 294.
(9) Zhou, X.-L.; White, J. M. *Catal. Lett.* **1989**, *2*, 375.
(10) Zhou, X.-L.; White, J. M. *J. Phys. Chem.* **1991**, *95*, 5575.
(11) Paul, A.; Bent, B. E. *Surf. Sci.* **1993**, *297*, 327.
(12) Paul, A.; Bent, B. E. *J. Catal.* **1994**, *147*, 264.
(13) Yang, Q. Y.; Johnson, A. D.; Maynard, K. J.; Ceyer, S. T. *J. Am. Chem. Soc.* **1989**, *111*, 8748.
(14) Fairbrother, D. H.; Peng, X. D.; Viswanathan, R.; Stair, P. C.; Trenary, M.; Fan, J. *Surf. Sci.* **1993**, *285*, L455.
(15) Laidler, K. J. *Chemical Kinetics*; Harper Collins Publishers: New York, 1987.
(16) Hammett, L. P. *Physical Organic Chemistry: Reaction Rates, Equilibria and Mechanisms*, 2nd ed.; McGraw-Hill: New York, 1970.
(17) Lewis, E. S. *Investigation of Rates and Mechanisms of Reactions: Part I*, 3rd ed.; John Wiley & Sons: New York, 1974; Chapter XIV.
(18) Jaffé, H. H. *Chem. Rev.* **1953**, *53*, 191.
(19) Taft, R. W. *Prog. Phys. Org. Chem.* **1983**, *14*, 247.
(20) Wells, P. R. *Linear Free Energy Relationships*; Academic Press Inc.: New York, 1968.
(21) Hansch, C.; Leo, A.; Taft, R. W. *Chem. Rev.* **1991**, *91*, 165.
(22) Chapman, N. B.; Shorter, J. *Advances in Linear Free Energy Relationships*; Plenum Press: London and New York, 1972.

0002-7863/95/1517-9056$09.00/0

constant. For example, the equilibrium constant for acetic acid deprotonation increases with successive substitution of hydrogen with fluorine in the methyl group since the carboxylate anion is increasingly stabilized compared to the neutral carboxylic acid by the electron withdrawing nature of fluorine, i.e. $pK_{a(CH_3COOH)} = 4.75$, $pK_{a(CH_2FCOOH)} = 2.66$, $pK_{a(CHF_2COOH)} = 1.24$, and $pK_{a(CF_3COOH)} = 0.23$.[23]

For reactions on metal surfaces, the choice of substituent groups for LFER studies is critical because of the close proximity of the metal surface to the reactant.[24] An ideal substituent group is one that only influences the reaction rate without changing the reaction mechanism. In the past, fluorine substituent effects have been successfully used to establish the charge separation in β-hydride elimination reactions of adsorbed alkoxides and alkyl groups on copper[25-27] and Ag(110)[28] surfaces and in the deprotonation reactions of carboxylic acids on Ag(110).[29,30] In these surface reactions fluorine proved to be an ideal substituent group. Its high electronegativity[23] has strong influence on the energetics of surface reactions involving polarized transition states, which translates into measurable changes in reaction rates observed during TPR studies. Moreover its small size ensures minimal steric interactions with the surface.[31] This study of fluorine substituent effects on the alkyl coupling reaction is part of our larger program to understand the nature of reaction centers in elementary surface reactions.

Most metal surfaces preferentially dehydrogenate adsorbed alkyl groups. Only under specific conditions, such as blocking of surface sites or at high coverages of reactant(s), can carbon–carbon bond formation reactions effectively compete with the dehydrogenation reactions. On Ag(111), however, alkyl groups only couple to form alkanes. Alkyl coupling reactions have been extensively studied by Zhou, White, and co-workers on the Ag(111) surface under UHV conditions.[8-10,32] Their studies show that the C–I bond in adsorbed alkyl iodides dissociates at temperatures below ~160 K on the Ag(111) surface to generate alkyl groups which then couple at temperatures between 175 and 260 K to yield alkanes. In our investigation of the coupling reactions of alkyl groups, Ag(111) was the surface of choice, as it is the only known surface which selectively exhibits the coupling reaction. Partially fluorinated alkyl groups were generated on the surface by the thermal dissociation of the C–I bond in the corresponding adsorbed alkyl iodides.

The coupling of adsorbed alkyl groups leading to the formation of a new carbon–carbon bond might be expected to be a symmetric reaction. Intuitively one would expect that even a strong electron withdrawing group like fluorine would not alter the rate of this reaction significantly. The results of this study, however, show a large decrease in reaction rate with fluorine substitution, indicating the involvement of a transition state which is electron deficient with respect to the initial state. It is interesting to note that in studies paralleling this one, we find that the energetics of phenyl coupling on the Cu(111) surface, also a symmetric reaction, exhibit the opposite influence of fluorine substitution in the phenyl ring.[33] The origin of this difference may lie in the difference in bonding of the alkyl and the phenyl group to metal surfaces and this is discussed in section 4.3.

2. Experimental Section

Experiments were conducted in two stainless steel ultra-high-vacuum (UHV) chambers. Most of the experiments were performed in the first chamber (hereafter referred to as chamber 1) which was equipped with an ion sputtering gun (Physical Electronics) and a retarding field analyzer (Physical Electronics) for both Auger electron spectroscopy (AES) and low-energy electron diffraction (LEED). In addition, residual gas analysis (RGA) and temperature programmed reaction (TPR) studies were performed with a quadrupole mass spectrometer (Ametek, Dycor M200M). This chamber was pumped with a cryopump (CTI-8) to a base pressure of $<4 \times 10^{-11}$ Torr.

The second chamber (chamber 2) is equipped with a sensitive quadrupole mass spectrometer (Extrel) and a differentially pumped ion gun (Perkin Elmer, 04-303). In the experiments described in this paper, the Extrel mass spectrometer was primarily used to identify the high molecular weight (>130 amu), partially fluorinated hydrocarbon products evolving from the surface during TPR studies. In addition, the chamber has capabilities for AES and LEED for surface characterization. The base pressure of this chamber is maintained at 2×10^{-10} Torr using an ion-pump (Physical Electronics) and a titanium sublimation pump.

The Ag(111) sample, 10 mm in diameter, was cut from a single crystal rod by electric discharge machining (EDM) so that one face of the sample was exposed to the (111) orientation (orientation off by ~3.5°). The surface was polished to a mirror finish by using a 0.05 μm alumina paste. The Ag(111) crystal was spotwelded between two Ta wires which were in thermal contact with two liquid nitrogen reservoirs. These Ta wires were also in electrical contact with a high current power supply for resistive heating of the sample. With this mounting scheme, sample temperatures of 95 to 1200 K were readily achieved. Temperature measurements were made with an alumel–chromel thermocouple junction pressed into a 0.01 in. diameter hole (drilled by the EDM method) at the edge of the Ag(111) crystal.

After the initial mounting and pumpdown, the surface was first cleaned by 3–4 cycles of Ar^+ ion sputtering at room temperature for 30 min and at 900 K for 5 min. Thereafter routine cleanliness (verified by AES) was obtained by sputtering at room temperature for 20 min, at 900 K for 3 min, and at room temperature for 15 min. During sputtering the Ar^+ beam voltage and current to the sample were typically between 2–4 kV and 4–6 μA, respectively. Surface order was recovered by annealing the sample to 950 K for 5 min and verified by LEED.

Controlled quantities of the reactants were adsorbed onto the surface by means of three separate leak valves, each ending in a capillary-array doser. During dosing, the sample was placed ~3 cm from the front of the doser and the leak valve opened to introduce the adsorbate into the chamber. The pressure of the adsorbate in the chamber, as measured by the ion gauge in this dosing geometry, multiplied by the dosing time constitutes our measurement of the exposure. Careful calibration of this dosing procedure shows that the exposure to the surface is typically 20–50 times larger than that obtained by backfilling the chamber to the same ambient pressure of the adsorbate. Exposures are reported in units of monolayer (ML), where one monolayer corresponds to the exposure required to achieve onset of multilayer desorption in TPR experiments. From calibration studies on Au(111), 1 ML typically corresponds to ~1 alkyl iodide molecule per 12 surface metal atoms.[11]

A major portion of the study described here was performed in chamber 1 where the quadrupole head of the mass spectrometer is covered in a protective stainless steel housing with a ~10 mm diameter aperture. During TPR studies, typically, the adsorbate covered sample is positioned in line of sight with and ~1–2 mm away from the aperture so that species desorbing selectively from the face of the crystal were

(23) Sheppard. W. A.; Sharts, C. M. *Organic Fluorine Chemistry*; W. A. Benjamin, Inc.: New York, 1969.
(24) Kraus. M. *Adv. Catal.* **1967**, *17*, 75.
(25) Gellman, A. J.; Dai, Q. *J. Am. Chem. Soc.* **1993**, *115*, 714.
(26) Forbes, J. G.; Gellman, A. J. *J. Am. Chem. Soc.* **1993**, *115*, 6277.
(27) Dai, Q.; Gellman, A. J. *J. Phys. Chem.* **1993**, *97*, 10783.
(28) Dai, Q.; Gellman, A. J. *J. Phys. Chem.* **1991**, *95*, 9443.
(29) Parker. B.; Gellman, A. J. *J. Am. Chem. Soc.* submitted for publication.
(30) Parker, B.; Zhang, R.; Dai, Q.; Gellman, A. J. In *Applications of Surface Science and Advances in Tribology*; Chung, Y., Homola, A. M., Street, G. B., Eds.; Am. Chem. Soc. Symp. Ser. No. 485; American Chemical Society: Washington, DC; Chapter 11.
(31) *CRC Handbook of Chemistry and Physics*; 70th ed.; CRC Press: Boca Raton, 1989–1990.
(32) Zhou, X.-L.; Blass, P. M.; Koel, B. E.; White, J. M. *Surf. Sci.* **1992**, *271*, 427.
(33) Meyers, J. M.; Gellman, A. J. *Surf. Sci.* In press.

detected by the quadrupole head of the mass spectrometer. The mass spectrometer was interfaced to a computer so that five ions could be monitored during a single TPR experiment. All mass spectra and TPR spectra acquired in this chamber were obtained with the mass spectrometer ionizer energy set at 70 eV. Heating rates of 0.1−10 K/s were obtained using a proportional and differential temperature feedback loop which was controlled by a computer.

TPR studies aimed specifically at identifying the high mass partially fluorinated hydrocarbon products were conducted in chamber 2. The Extrel mass spectrometer in this chamber is more sensitive than the Dycor mass spectrometer in chamber 1 and was primarily operated at a lower ionizer energy of 33 eV to reduce the extent of fragmentation of the partially fluorinated hydrocarbons and to aid in the detection of the parent and/or large daughter ions. The quadrupole head of the 10″ long Extrel mass spectrometer, shielded in a stainless steel casing, ends in an axial ionizer (041-11) which has an aperture (2 mm diameter) at the center. During TPR studies the surface was placed ~5 mm in front of this aperture and up to three masses could be monitored during a single desorption run. However, to enhance the signal-to-noise ratio for TPR spectra collected at 33 eV, only one mass was monitored for each desorption experiment.

Ethyl iodide (99% purity) was obtained from the Aldrich Chemical Co., and propyl iodide (97% pure) and trifluoropropyl iodide (95% pure) were purchased from Lancaster Synthesis. All the above liquid samples are light sensitive and were initially purified through a column of basic alumina to remove any acidic impurity such as HI and I_2 formed as a result of photochemical degradation. Thereafter further decomposition of these alkyl iodides was prevented by storing them in shielded glass vials. Dissolved gases were removed by several cycles of freeze−pump−thaw prior to their use in the UHV system. Argon gas (prep. grade) was purchased from Matheson.

3. Results

We present the results of our experiments in three sections. First, results of the coupling reaction of unsubstituted alkyl groups (ethyl and propyl) will be discussed along with the determination of the reaction rate parameters. The effect of fluorine substitution on the coupling of adsorbed alkyl groups was investigated by using $CF_3CH_2CH_{2(ad)}$ and is presented in section 3.2. It is worth mentioning here $CF_3CH_{2(ad)}$ and $CF_3CF_2CH_{2(ad)}$ do not dimerize but instead β-fluoride eliminate at temperatures below 300 K to generate $CF_2{=}CH_2$ and $CF_3CF{=}CH_2$, respectively.[34] Therefore it was not possible to investigate the effects on the alkyl coupling reaction of fluorine substitution at the β-carbon position. Finally, in section 3.3, cross-coupling reactions between (a) coadsorbed $CH_3CH_{2(ad)}$ and $CF_3CH_2CH_{2(ad)}$ and (b) coadsorbed $CH_3CH_2CH_{2(ad)}$ and $CF_3CH_2CH_{2(ad)}$ are presented.

3.1. Coupling of $CH_3CH_{2(ad)}$ Groups and $CH_3CH_2CH_{2(ad)}$ Groups. Extensive studies by X.-L. Zhou, J. M. White, and co-workers have established that adsorbed alkyl groups, both linear and branched, dimerize on the Ag(111) surface to yield alkanes of twice the chain length.[8−10,32] Consistent with their findings, our studies of CH_3CH_2I and $CH_3CH_2CH_2I$ on a Ag(111) surface show the evolution of $CH_3(CH_2)_2CH_3$ and $CH_3(CH_2)_4CH_3$ respectively as the reaction products. Figure 1 shows the evolution of butane after an exposure of 0.17 ML of ethyl iodide on the Ag(111) surface, detected by monitoring the signal at m/e = 58 for heating rates between 0.2 and 10 K/s. The evolution of hexane (m/e = 57 fragment) from the reaction of 0.2 ML of n-propyl iodide during TPR studies performed at heating rates between 0.2 and 5 K/s is shown in Figure 2. The cracking patterns of both products in our mass spectrometer are consistent with the standard mass spectra reported in the literature.[35] The evolution of the alkane products

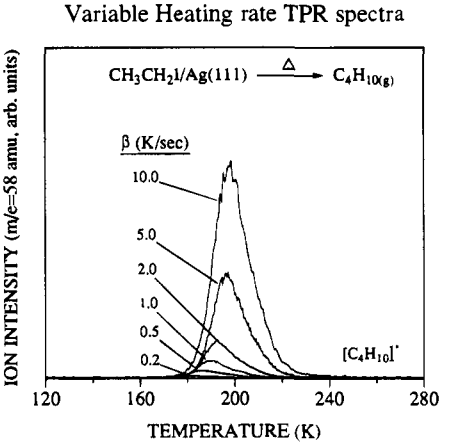

Figure 1. TPR spectra showing the evolution of butane after the reaction of CH_3CH_2I on the Ag(111) surface for heating rates (β) between 0.2 and 10 K/s. The initial coverage was determined based on the exposure required to observe the onset of CH_3CH_2I multilayer desorption.

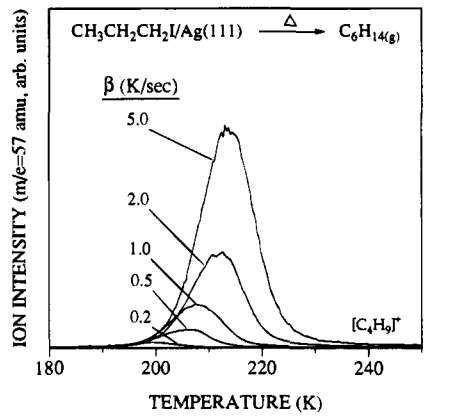

Figure 2. Hexane evolution after the reaction of 0.2 ML of $CH_3CH_2CH_2I$ on the Ag(111) surface for heating rates (β) between 0.2 and 5 K/s. The coverage was determined from the exposure required to observe the onset of $CH_3CH_2CH_2I$ multilayer desorption.

is rate-limited by the recombination of the corresponding adsorbed alkyl groups as has been demonstrated in ref 10.

For a constant initial coverage of the reactant, variable heating rate TPR experiments provide a way to determine the coverage-independent kinetic parameters, activation energy (E_a), and pre-exponential factor (ν).[36,37] The recombination of alkyl groups (ethyl and propyl), a bimolecular reaction, does not exhibit the behavior normally expected of second-order reactions during coverage-dependent TPR studies.[36] This is attributed to interactions between the adsorbed reactants.[9,10] Further, at coverages near saturation, the dissociation of the C−I bond in ethyl iodide on the Ag(111) surface is sterically hindered and occurs over a broad range of temperatures encompassing the coupling reaction temperature.[9] In order to minimize any of these coverage-dependent complications it is desirable to perform variable heating rate TPR studies at low exposures. This was the case in Figures 1 and 2 where the initial coverages of ethyl and propyl groups were 0.17 and 0.2 ML, respectively. The TPR peak temperatures (T_p) in Figures 1 and 2 increase with increasing heating rates (β) and these values were used to plot log (β/T_p^2) vs $1/T_p$ in Figure 3. The data for the recombination of

(34) Paul, A.; Gellman, A. J. *Langmuir*. Submitted for publication.
(35) Heller, S. R.; Milne, G. W. A. *EPA/NIH Mass spectral Data Base*. 1978.
(36) Redhead, P. A. *Vacuum* **1962**, *12*, 203.
(37) Miller, J. B.; Siddiqui, H. R.; Gates, S. M.; Russell, J. N.; J. T. Yates, J.; Tully, J. C.: Cardillo, M. J. *J. Chem. Phys.* **1987**, *87*, 6725.

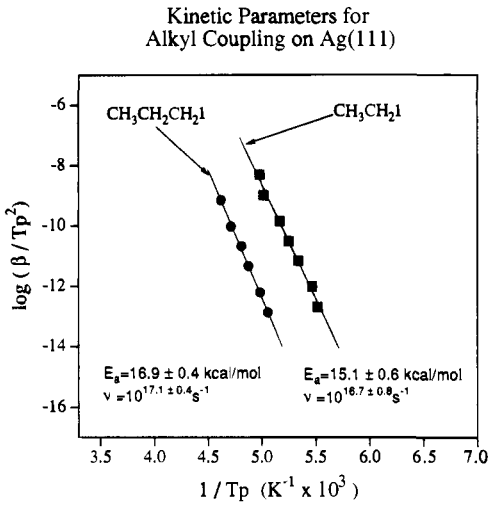

Figure 3. Plot of log (β/T_p^2) vs $1/T_p$ for the coupling of ethyl and propyl groups on the Ag(111) surface. TPR peak temperatures (T_p) as a function of the heating rates (β) were obtained from the variable heating rate TPR studies in Figures 1 and 2. The slope of the least-squares line fit to the data yields the activation energy for each reaction. Pre-exponential factors were determined by substituting the values of E_a in a first-order rate expression. The values of E_a and ν are shown in the figure below each plot.

$CH_3CH_{2(ad)}$ are represented as solid squares and that for $CH_3CH_2CH_{2(ad)}$ as solid circles. The slope of the lines fit to the data in Figure 3 yield $E_a = 15.1 \pm 0.6$ kcal/mol for the coupling of $CH_3CH_{2(ad)}$ and $E_a = 16.9 \pm 0.4$ kcal/mol for the coupling of $CH_3CH_2CH_{2(ad)}$.[36] Since the absolute coverages of $CH_3CH_{2(ad)}$ or $CH_3CH_2CH_{2(ad)}$ in these experiments were undetermined, pseudo-first-order pre-exponential factors are evaluated by substituting the above activation energies into the first-order rate expression and were found to be $10^{16.7\pm0.8}$ and $10^{17.1\pm0.4}$ s^{-1}, respectively.

The surface step density is 1 step atom every ~40 terrace atoms (i.e. surface oriented to within 3.5° to the (111) surface). Based on the calibration of alkyl iodides on Au(111)[11] and the fact that Au and Ag have similar van der Waal radii, we estimate that the absolute coverage of physisorbed alkyl iodides at 0.2 ML is ~1 molecule per ~60 surface Ag atoms, which is comparable to the density of step sites. Thus at these low coverages, it is probable that the coupling reaction takes place at step edges. In fact for the coupling of $CH_3CH_{2(ad)}$, there is a TPR peak at ~210 K, which we believe is due to reaction at defect sites since it saturates at a very low coverage of ~0.02 ML. For exposures >0.02 mL this "defect site" TPR peak appears as a high-temperature shoulder to the major TPR peak (see for example the high-temperature shoulder in Figure 1). For $CH_3CH_2CH_{2(ad)}$ there is only one distinct TPR peak at all coverages below 1 ML. Thus, it appears that defect sites, such as step edges, do not affect the coupling temperature of alkyl groups. One probable reason is that once the C−I bond dissociates the surface iodine preferentially bonds to and blocks the step edges, leaving terrace sites for the coupling reaction.

3.2. Reactions of $CF_3CH_2CH_{2(ad)}$. Unlike the simple recombination reactions of $CH_3CH_{2(ad)}$ and $CH_3CH_2CH_{2(ad)}$, the reaction of $CF_3CH_2CH_{2(ad)}$ on the Ag(111) surface appears to be quite complex. This is illustrated in Figure 4A where five fragments were monitored in a multiplexed TPR experiment for a 0.17 ML coverage of $CF_3CH_2CH_2I$. At this low coverage there is clear evidence of two reactions, one occurring at ~300 K, contributing primarily to m/e = 96 and 69 signals, and the other at ~280 K, contributing to signals at 47, 64, 69, and 110 amu.

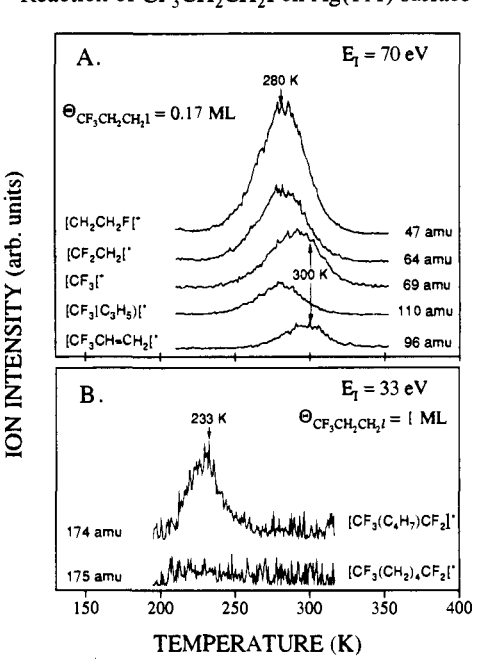

Figure 4. (A) TPR spectra monitored at β = 2 K/s for selected fragments after exposing the Ag(111) surface to 0.17 ML of $CF_3CH_2CH_2I$. This exposure was based on a comparison of the iodine coverage deposited on the surface after this TPR experiment and that for a saturation exposure TPR experiment. The mass spectrometer ionizer energy (E_I) was 70 eV. Section 3.2 discusses the products evolving from the surface at 280 and 300 K. (B) The evolution of the coupling product, $CF_3(CH_2)_4CF_3$, during TPR studies for a saturation exposure of $CF_3CH_2CH_2I$ on the Ag(111) surface. The representative ions are $CF_3(C_4H_7)CF_2^+$ and $CF_3(CH_2)_4CF_2^+$ at m/e = 174 and 175, respectively, monitored at E_I = 33 eV. The ratio of the signals at m/e = 174:175 is ~6:1. At coverages of $CF_3CH_2CH_{2(ad)}$ high enough (>0.6 ML) that m/e = 174 and 175 signals are detectable, the TPR profile of the signal at m/e = 110 ($CF_3(C_3H_5)^+$) is identical to those of m/e = 174 and 175.

Table 1. Relative Mass Spectrometric Ion Intensities of Selected Fragments with Respect to the m/e 69 amu Fragment of Each Molecule

daughter ions	parent molecule			
(m/e in amu)	CF_3CH_2I	$CF_3CH_2CH_2I$	$CF_3CF_2CH_2I$	$CF_3CH{=}CH_2$
47		28	1	5
64	204	4	79	3
69	100	100	100	100
77		212	5	202
95		44	17	147
96		36	1	127
97		43		

The reaction at 300 K is a minor reaction pathway and saturates at very low exposures, typically below 0.05 ML. From the ratio of the intensities at m/e = 96, 95, and 69 (at <0.05 ML exposures) the product at this temperature has been identified as $CF_3CH{=}CH_2$ (see Table 1). The evolution of $CF_3CH{=}CH_2$ is probably limited by β-hydride elimination reaction at defect sites and/or desorption from defect sites. The fate of the resulting H atom on the Ag(111) surface is not certain as the intensities of the reductive elimination product, $CF_3CH_2CH_3$ (mol wt 98 amu) and/or molecular H_2 (mol wt 2 amu), were below the detection limits of the mass spectrometer. It is already known that surface H recombines on this surface at temperatures below 200 K.[38]

(38) Zhou, X.-L.; White, J. M.; Koel, B. E. *Surf. Sci.* **1989**, *218*, 201.

Unfortunately the analysis of the product(s) formed at 280 K, the major reaction pathway, is not straightforward. A complete analysis is hampered in part because only a very limited number of mass spectra of partially fluorinated alkanes are reported in the literature[35] and partly because the hydrofluorocarbons readily fragment and rearrange[39-41] inside the mass spectrometer.

Nevertheless, certain products are easily identifiable. In particular, if $CF_3CH_2CH_{2(ad)}$ were to dimerize as ethyl and propyl groups do, ionization of the resulting product, $CF_3(CH_2)_4CF_3$, would give rise to fragments with chain lengths greater than three carbon atoms. The *m/e* = 110 fragment in Figure 4A represents a four-carbon ion ($CF_3(CH_2)_2CH^+$) and is most likely a cracking fragment of the recombination product, $CF_3(CH_2)_4CF_3$. At this low coverage, ions having *m/e* ratios greater than 110 were not readily detected by the mass spectrometer, but at higher coverages (>0.6 ML), $CF_3(CH_2)_3CH^+$ (*m/e* = 124), $CF_3(CH_2)_3CH_2^+$ (*m/e* = 125), $CF_3(CH_2)_4C^+$ (*m/e* = 137), $CF_3(CH_2)_4CF^+$ (*m/e* = 156), $CF_3(C_4H_7)CF_2^+$ (*m/e* = 174), and $CF_3(CH_2)_4CF_2^+$ (*m/e* = 175) were observed and gave TPR profiles identical to the TPR profiles of the $CF_3(CH_2)_2CH^+$ fragment (*m/e* = 110), at all coverages. The largest fragment detected was $CF_3(CH_2)_4CF_2^+$ (*m/e* = 175), and it is shown in Figure 4B for a saturation exposure of $CF_3CH_2CH_2I$. Note that the mass spectrometer ionizer energy in Figure 4B was reduced to 33 eV to decrease the extent of fragmentation of the hexafluorohexane molecule in the mass spectrometer. Even then, the signal-to-noise ratio is far better for *m/e* = 174 ($CF_3(C_4H_7)CF_2^+$), the fragment with a mass 20 amu lower than the mass of the parent molecule, than it is for *m/e* = 175 ($CF_3(CH_2)_4CF_2^+$), the fragment with mass 19 amu lower than the mass of the parent molecule. The signal of the parent molecule, $CF_3(CH_2)_4CF_3$ (mol wt 194 amu), was below the detection limits of the mass spectrometer. An important observation from Figure 4 is that the coupling temperature of $CF_3CH_2CH_{2(ad)}$ decreases with increasing coverage, starting at ~280 K for submonolayer exposures (*m/e* = 110 spectra in Figure 4A) and decreasing to ~230 K for saturation exposures (*m/e* = 174 spectra in Figure 4B).

An assessment of the characteristics of fragmentation patterns of CF_3-terminated alkanes could not be made due to the lack of a mass spectrometric data base for CF_3-terminated alkanes in the literature. Fortunately however, the mass spectrometric data base for CF-terminated alkanes (i.e. $CFH_2(CH_2)_nCH_3$) is quite extensive (n = 0 to 5) and can be used as a guide to understanding the fragmentation of the large chain hydrofluoroalkanes.[35] The general trends in the mass spectrometric *intensities* of the $CFH_2(CH_2)_nCH_3$ series of alkanes is as follows: the *intensity* of the fragment with mass 20 amu less than the mass of the parent alkane, formed by HF elimination (i.e. $(C_nH_{2n-1})CH_3^+$), is greater than the *intensity* of the fragment with a mass 19 amu less than the parent molecular weight, formed by F elimination (i.e. $(C_nH_{2n})CH_3^+$), which in turn is greater than the *intensity* of the parent ion. The mass spectrum of $CF_3(CH_2)_4CF_3$ also shows similar behavior, as discussed above and seen in Figure 4B. Examples of similar fragmentation in the mass spectrum of the $CF_3(CH_2)_nCH_3$ series of hydrofluoroalkanes (n = 3 and 4) are discussed in section 3.3. These observations are also consistent with the general characteristics of the mass spectra of hydrohalocarbons discussed in ref 41, where elimination of HX is argued to be energetically favored over the elimination of X, when X is either Cl or F.

Besides the coupling product, $CF_3(CH_2)_4CF_3$, there is evidence for the formation of other products at the same temperature. In particular, the intensity of the *m/e* = 64 fragment ($CF_2CH_2^+$) at 280 K is greater than that of the *m/e* = 69 fragment (CF_3^+) by a factor of ~1.7 (this ratio is obtained after subtracting contributions due to the 300 K peak), which is quite unusual. Our previous experience with a number of CF_3-terminated alkyl iodides, hydrocarbons, and alcohols has shown that the intensity of the CF_3^+ ion (*m/e* = 69) is almost always greater than that of the $CF_2CH_2^+$ ion (*m/e* = 64). The only exception is CF_3CH_2I, where presumably the preferred elimination of FI from adjacent carbon atoms causes the intensity at *m/e* = 64 to be greater than that at *m/e* = 69 (Table 1). For example, the ratio of *m/e* 64:69 intensities is 0.04 in $CF_3CH_2CH_2I$, 0.03 in $CF_3CH{=}CH_2$, and 0.79 in $CF_3CF_2CH_2I$ (see Table 1). This is also borne out by the standard mass spectrum of CF_3CH_3 where the ratio of the intensities of *m/e* 64:69 signals is 0.17.[35] A rational explanation for the observed *m/e* = 64 and 69 intensities in Figure 4A is that one of the products at 280 K has a $-CF_2CH_2-$ unit and probably lacks a terminal CF_3 group. In this regard it is interesting to note that $CF_3CF_2CH_2I$, which has both a terminal CF_3 group and a $-CF_2CH_2-$ unit, shows an *m/e* 64:69 intensity ratio equal to 0.79 (Table 1), which is significantly greater than the ratio of 0.04 for $CF_3CH_2CH_2I$ (which has only a terminal CF_3 group).

In addition, the $CH_2CH_2F^+$ ion (*m/e* = 47) in the TPR spectra of Figure 4A is more intense than all other fragments (e.g. *m/e* 47:69 ratio is 3:1). Although the $CH_2CH_2F^+$ ion often arises due to electron induced rearrangement of hydrofluorocarbons in the mass spectrometer,[39] its strong intensity in Figure 4A is quite unexpected. As a guide, the ratio of the intensity for *m/e* = 47 to 69 is 0.28 in the mass spectrum of $CF_3CH_2CH_2I$ (Table 1).

Apart from the unusual TPR intensities for *m/e* = 64 and 47 in the reaction of $CF_3CH_2CH_{2(ad)}$ on Ag(111), we were also able to detect trace amounts of AgF desorption from the surface indicating some γ C−F bond dissociation on the Ag(111) surface. The results are shown in Figure 5. Clean Ag(111) sublimes Ag atoms at temperatures above 800 K, as seen in the TPR spectra (a) of Figure 5A. When the same surface is exposed to a large dose (>3 ML) of $CF_3CH_2CH_2I$ at 270 K, the *m/e* = 107 TPR spectra shows enhanced desorption around 850 K. The difference between the TPR spectra for the surface dosed with $CF_3CH_2CH_2I$ (i.e. plot (b), Figure 5A) and the TPR spectra for the clean Ag(111) surface (i.e. plot (a), Figure 5A) is shown in Figure 5B. The spectra in Figure 5B shows a distinct peak at ~850 K. Based on the β-fluoride elimination studies in ref 34, where F chemisorbed on the Ag(111) surface was found to desorb as AgF at ~850 K, we attribute the peak in Figure 5B to AgF desorption from the surface. The signals for the F^+ ion (*m/e* = 19) and the AgF^+ ion (*m/e* = 126) corresponding to the signal for the Ag^+ ion (*m/e* = 107) in Figure 5B were below the detection limits of the mass spectrometer. This mass spectrometric intensity behavior is consistent with the fragmentation pattern of AgF observed in ref 34 where the *m/e* 107:19:126 ratio was found to be ~23:1:1.8. Judging from the TPR peak area for AgF desorption at 850 K in Figure 5B, the amount of F deposited on the Ag(111) surface by dosing >3 ML of $CF_3CH_2CH_2I$ at ~270 K is very low. For a comparison, using similar dosing procedures, the *m/e* = 107 TPR peak area for AgF desorption from a surface dose with CF_3CH_2I (which β-fluoride eliminates at ~250 K[34])

(39) McLafferty, F. W. *Mass Spectral Correlations*; American Chemical Society: Washington, DC, 1963.
(40) *Advances in Fluorine Chemistry*; Stacey, M., Tatlow, J. C., Sharpe, A. G., Eds.: Butterworths: Washington, DC, 1961; Vol. 2, pp 55−103.
(41) Shrader, S. R. *Introductory Mass Spectrometry*; Allyn and Bacon, Inc.: Boston, 1971.

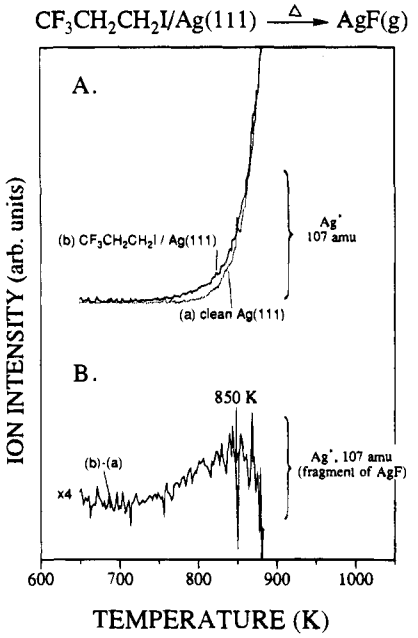

Figure 5. TPR spectra at m/e = 107 (Ag^+). (A) Clean Ag(111) sublimes Ag atoms above 800 K, shown in plot (a) as a dotted line. When the same surface is exposed to >3 ML dose of $CF_3CH_2CH_2I$ at 270 K, the m/e = 107 TPR spectra shows an enhanced desorption feature ~850 K, seen in (b), the solid line plot. (B) The difference spectra, (a)−(b), shows a peak at 850 K attributed to desorption of AgF from the surface.

is ~8.3 times greater than that obtained by using $CF_3CH_2CH_2I$ as in Figure 5.

The results in Figures 4 and 5 indicate that apart from the coupling product, $CF_3(CH_2)_4CF_3$, there are other products formed at 280 K. As discussed above, the source of the large m/e = 64 intensity in the mass spectrometer is most likely from a product which has a $-CF_2CH_2-$ unit. In addition a trace amount of F is deposited on the Ag(111) surface. One possible reaction that can account for the above-mentioned observations is shown below (reaction 1):

$$CF_3CH_2CH_{2(ad)} \rightarrow \overline{CH_2CF_2CH_2} + F_{(ad)} \qquad (1)$$

Reaction 1 involves dissociation of the γ C−F bond in $CF_3CH_2CH_{2(ad)}$ resulting in chemisorbed F on the Ag(111) surface and the evolution of the difluorocyclopropane, $\overline{CH_2CF_2CH_2}$, from the surface. The source of the large m/e = 64 signal in Figure 4A is fragmentation of the $\overline{CH_2CF_2CH_2}$ product to the $CF_2CH_2^+$ ion in the mass spectrometer. The origin of the large signal for $CH_2CH_2F^+$ ion (m/e = 107) is most likely as a result of electron induced rearrangement of the products $\overline{CH_2CF_2CH_2}$ and $CF_3(CH_2)_4CF_3$ in the mass spectrometer.[39,40] Chemisorbed F desorbs as AgF at ~850 K. From the small amount of F deposited on the surface after the reaction of $CF_3CH_2CH_{2(ad)}$, we conclude that the γ C−F dissociation reaction (reaction 1) is a minor reaction channel compared to the coupling reaction discussed earlier in this section which yields $CF_3(CH_2)_4CF_3$.

It is important to note that because the fragmentation pattern of the partially fluorinated hydrocarbon products discussed above is unknown, and because their mass spectra can give rise to the same cracking fragments, the analysis above is by no means complete. We therefore do not eliminate the possibility of other and/or different reaction products. In particular, the γ-fluorine elimination reaction (reaction 1) is

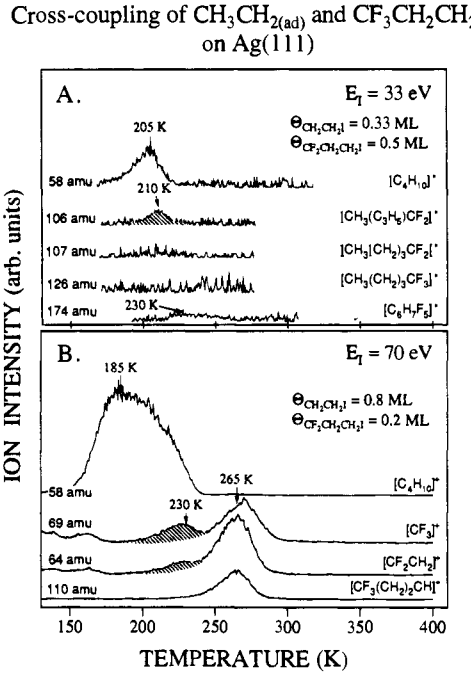

Figure 6. Coadsorption studies of $CH_3CH_{2(ad)}$ and $CF_3CH_2CH_{2(ad)}$ on the Ag(111) surface demonstrating the evolution of the cross-coupling product, $CF_3(CH_2)_3CH_3$, represented by the shaded peaks. The heating rate is 2 K/s. (A) T_p is ~210 K in the TPR spectra of m/e = 106 and 107 fragments ($CF_2(C_3H_5)CH_3^+$ and $CF_2(CH_2)_3CH_3^+$ respectively) at a mass spectrometer ionizer energy (E_I) of 33 eV. High initial coverages of $CH_3CH_{2(ad)}$ and $CF_3CH_2CH_{2(ad)}$ (i.e. 0.33 and 0.5 ML, respectively) were used to aid in the detection of the signals of all the coupling products (or their large daughter ions). (B) T_p is 230 K for m/e = 69 and 64 fragments (CF_3^+ and $CF_2CH_2^+$ ions, respectively) monitored at E_I = 70 eV. A high initial coverage of $CH_3CH_{2(ad)}$ (i.e. 0.8 ML) ensures that even though $CH_3CH_{2(ad)}$ is rapidly consumed via the self-coupling reaction at 185 K, its coverage at the cross-coupling reaction temperature is comparable to the coverage of $CF_3CH_2CH_{2(ad)}$ (i.e. 0.2 ML) on the surface. The ratio of the intensities of ions at m/e 69:64 for the 230 K peak is 2.0.

unprecedented and to the best of our knowledge does not occur in gas or solution phase chemistry of organometallic compounds.[23,42] However, we are confident of the formation of the coupling product, $CF_3(CH_2)_4CF_3$, as fragments with six carbon chain lengths were detected.

The evolution of the gas-phase product $CF_3(CH_2)_4CF_3$ is probably limited by reaction on the surface and not by its desorption. A direct measurement of the molecular desorption temperature could not be made as $CF_3(CH_2)_4CF_3$ is not commercially available. However, on copper and silver surfaces, fluorine substitution for hydrogen in the alkyl chains of alcohols decreases the molecular desorption temperatures by ~10 K.[27] Based on this trend, the molecular desorption temperature of $CH_3(CH_2)_4CH_3$ from the Ag(111) surface, which occurs below 190 K,[10] is expected to be lowered as a result of fluorination of the terminal CH_3 groups.

3.3. Cross-Coupling Reactions. When two dissimilar alkyl groups are coadsorbed on the Ag(111) surface they cross-couple as demonstrated below for two cases: (a) coadsorbed CH_3CH_2 and $CF_3CH_2CH_2$ groups and (b) coadsorbed $CH_3CH_2CH_2$ and $CF_3CH_2CH_2$ groups.

3.3.1. Cross-Coupling between $CH_3CH_{2(ad)}$ and $CF_3CH_2CH_{2(ad)}$. Figure 6 shows the TPR results, at selected masses, for the cross-coupling studies between coadsorbed $CH_3CH_{2(ad)}$ and $CF_3CH_2CH_{2(ad)}$. For clarity, the TPR peaks corresponding

(42) Banks, R. E. *Fluorocarbons and their Derivatives*, 2nd ed.; MacDonald & Co. Ltd.: London, 1970.

Table 2. Values of Kinetic Parameters and the Substituent Constants Used to Construct LFER Plots

reaction	substituent group(s) (X)	substituent[a] constant (σ_i)$_X$	$\sum_j(\sigma_i)_{X_j}$	Tp at β = 2 K/s [K]	pre-exponent factor (log ν [s^{-1}])	activation energy (E_a) [kcal/mol]	log k at 300 K
$(CH_3)_2CH + (CH_3)_2CH$	4-CH_3-	−0.05	−0.2	185[b]	16.7 ± 0.4[c]	14.4 ± 0.3[d]	6.2
$CH_3CH_2 + CH_3CH_2$	2-CH_3-	−0.05	−0.1	193	16.7 ± 0.8[e]	15.1 ± 0.6[e]	5.7
$CH_3CH_2CH_2 + CH_3CH_2CH_2$	2-CH_3CH_2-	−0.05	−0.1	212	17.1 ± 0.4[e]	16.9 ± 0.4[e]	4.8
$CH_3 + CH_3$	2-H-	0	0	150[f]	16.3 ± 0.4[c]	19.0 ± 0.4[d]	2.5
$CH_3CH_2CH_2 + CF_3CH_2CH_2$	H_3CH_2- / CF_3CH_2-	−0.05 / 0.15	0.1	220[g]	17.8[c]	18.3[h]	4.4
$CH_3CH_2 + CF_3CH_2CH_2$	CH_3- / CF_3CH_2-	−0.05 / 0.15	0.1	230[g]	17.5 ± 0.1[c]	18.9 ± 0.1[h]	3.7
$CF_3CH_2CH_2 + CF_3CH_2CH_2$	2-CF_3CH_2-	0.15	0.3	280	18.3[c]	24.2[h]	0.7

[a] Reference 21. [b] β = 2.5 K/s, ref 10. [c] Extrapolated from the values of ethyl and propyl coupling by assuming a "loose" transition state (the new C−C bond length in the transition state is unknown but is assumed to be between the sum of the covalent and the sum of the Van der Waals radius of carbon; this is shown as the ± value in ν here): this work. [d] Calculated from T_p of studies in ref 8 and 10 and the value of ν^* in this work. [e] From variable heating rate TPR studies, this work. [f] β = 3 K/s, ref 8. [g] From TPR results at a high initial coverage of alkyl and a low coverage of $CF_3CH_2CH_2$ group on the Ag(111) surface, this work. [h] Calculated from T_p and ν^*, this work.

to the evolution of the cross-coupling product, $CF_3(CH_2)_3CH_3$, are shaded in these spectra. The TPR spectra in Figure 6A were monitored at an electron impact energy of 33 eV to reduce the extent of fragmentation of the parent molecules in the mass spectrometer and to demonstrate the existence of the cross-coupling product, $CF_3(CH_2)_3CH_3$. The coverages of $CH_3CH_{2(ad)}$ and $CF_3CH_2CH_{2(ad)}$ in Figure 6A are high, i.e. 0.33 and 0.5 ML, respectively, to optimize the detection of all the coupling products (or their large daughter fragments). Apart from the self-coupling reaction (coupling between two similar alkyl groups) of $CH_3CH_{2(ad)}$ at 205 K resulting in butane (*m/e* = 58) and the self-coupling reaction of $CF_3CH_2CH_{2(ad)}$ at 230 K forming $CF_3(CH_2)_4CF_3$ (*m/e* = 174), there is a distinct signal at 210 K for *m/e* = 106. The *m/e* = 106 ion is $CH_3(C_3H_5)$-CF_2^+, and it is a cracking fragment with a mass 20 amu less than the mass of the cross-coupling product, $CH_3(CH_2)_3CF_3$ (mol wt 126 amu). As discussed in section 3.2, it is characteristic for CF_3-terminated alkanes to fragment in the mass spectrometer such that the intensity of the parent ion signal is lower than that of the fragment with mass 19 amu (i.e. mass of F) less than the parent alkane, which in turn is lower than the intensity of the signal for the fragment with mass 20 amu (i.e. mass of HF) less than the mass of the parent alkane.[38,41] The cross-coupling product, $CF_3(CH_2)_3CH_3$, formed at 210 K in Figure 6A also shows similar fragmentation. The signal of the parent ion, $CF_3(CH_2)_3CH_3^+$ (*m/e* = 126), in Figure 6A, is below the detection limit of the mass spectrometer and the signal of the *m/e* = 107 fragment, $CF_2(CH_2)_3CH_3^+$, is barely visible at 210 K. On the other hand, the signal for the *m/e* = 106 ion, CF_2-$(C_3H_5)CH_3^+$ in Figure 6A, is very distinct at 210 K.

The rate of the cross-coupling reaction depends not only on its intrinsic kinetic parameters, E_a and ν, but also on the coverage of each of the reactants, $CH_3CH_{2(ad)}$ and $CF_3CH_2CH_{2(ad)}$ on the Ag(111) surface. Therefore, if the TPR peak temperature of this reaction is to be used to extract the kinetic parameters, it is important to take care that the coverage of both reactants is comparable at the reaction temperature. The $CH_3CH_{2(ad)}$ groups self-couple at a much faster rate (lower temperatures) than they cross-couple with coadsorbed $CF_3CH_2CH_{2(ad)}$, so that during a TPR run, such as in Figure 6A, where the initial coverages of $CH_3CH_{2(ad)}$ and $CF_3CH_2CH_{2(ad)}$ are comparable, a major fraction of the $CH_3CH_{2(ad)}$ coverage is consumed via the self-coupling pathway. Under these initial conditions, the rate of the cross-coupling reaction drops rapidly due to the diminishing coverage of $CH_3CH_{2(ad)}$, giving a lower limit of the cross-coupling TPR peak temperature. A reliable determination of the cross-coupling temperature can be made if the initial coverage of CH_3-$CH_{2(ad)}$ is kept high and that of $CF_3CH_2CH_{2(ad)}$ kept low. With these initial conditions, the coverages of both reactants at the reaction temperature will be comparable and the TPR peak temperature would reflect a more accurate value of the kinetic parameters. The results of such an experiment are shown in Figure 6B where the initial coverages of $CH_3CH_{2(ad)}$ and CF_3-$CH_2CH_{2(ad)}$ are 0.8 and 0.2 ML, respectively. The cross-coupling TPR peak is represented by the shaded area for signals at 69 and 64 amu. Note that the cross-coupling peak temperature at 230 K in Figure 6B is 20 K higher than in Figure 6A, for reasons explained above. The 230 K cross-coupling reaction temperature is tabulated in column 5 of Table 2 and is used to evaluate the reaction rate constant. In Figure 6B more intense fragments were monitored with a mass spectrometer ionizer energy of 70 eV for a better signal-to-noise ratio. It is interesting to note here that the signal for *m/e* = 69 (CF_3^+) is more intense than the signal for *m/e* = 64 ($CF_2CH_2^+$), as would be expected for a CF_3-terminated cross-coupling product, $CF_3(CH_2)_3CH_3$. Although it is not shown here, the intensity of the $CH_2CH_2F^+$ ion (*m/e* = 47) at 230 K is ~3.8 times greater than that of the CF_3^+ ion (*m/e* = 69), consistent with the discussion in section 3.2, where it was suggested that the $CH_2CH_2F^+$ ion is readily formed by electron induced rearrangement of hydrofluorocarbons in the mass spectrometer.[39,40]

3.3.2. Cross-Coupling between $CH_3CH_2CH_{2(ad)}$ and CF_3-$CH_2CH_{2(ad)}$. The results in this section are presented on the same lines of reasoning as in section 3.3.1. The TPR results of coadsorption studies between $CH_3CH_2CH_{2(ad)}$ and CF_3CH_2-$CH_{2(ad)}$ on the Ag(111) surface in Figure 7A show the evolution of the cross-coupling product, $CF_3(CH_2)_4CH_3$, at 217 K characterized by the signals at *m/e* = 120 ($CF_2(C_4H_7)CH_3^+$) and 121 ($CF_2(CH_2)_4CH_3^+$). In addition, we observe the formation of the self-coupling products $CH_3(CH_2)_4CH_3$ (*m/e* = 86) at 213 K and $CF_3(CH_2)_4CF_3$ (*m/e* = 174) at 260 K. The intensity of the fragments at *m/e* = 120 and 121, which are fragments having masses 20 and 19 amu lower than the mass of the parent product, $CF_3(CH_2)_4CH_3$ (mol wt 140 amu), is characteristic of the mass spectrum of CF_3-terminated long-chain alkanes as discussed in sections 3.2 and 3.3.1. Note that the mass spectrometer ionizer energy in Figure 7A was 33 eV, and the initial coverage of both reactants was high (i.e. 0.5 ML of $CH_3CH_2CH_{2(ad)}$ and 0.33 ML of $CF_3CH_2CH_{2(ad)}$) to aid in the detection of the parent and/or large daughter ions of all the coupling products. Even then the evolution of the $CF_3(CH_2)_4$-CF_3 product, represented by *m/e* = 174, was below the mass spectrometer detection limit. For clarity the cross-coupling TPR peaks are shaded in Figures 7A and 7B.

As in the case of the cross-coupling studies of $CH_3CH_{2(ad)}$ and $CF_3CH_2CH_{2(ad)}$ discussed in section 3.3.1, the cross-coupling temperature between $CH_3CH_2CH_{2(ad)}$ and $CF_3CH_2CH_{2(ad)}$ is a function of the reactant coverage at the reaction temperature.

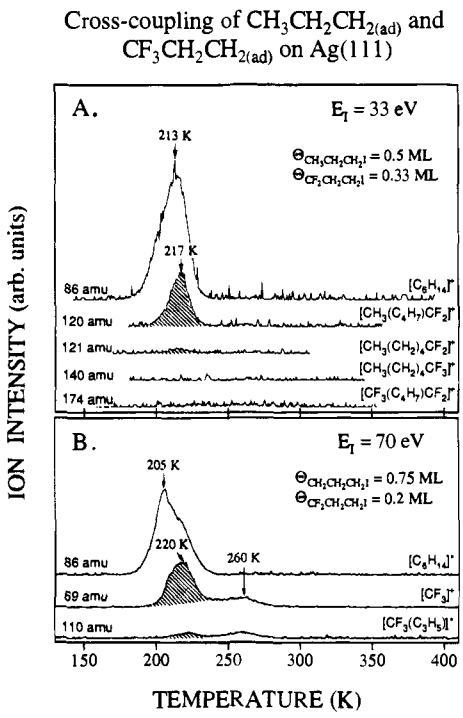

Figure 7. Coadsorption studies of $CH_3CH_2CH_{2(ad)}$ and $CF_3CH_2CH_{2(ad)}$ on the Ag(111) surface similar to the coadsorption studies of $CH_3CH_{2(ad)}$ and $CF_3CH_2CH_{2(ad)}$ in Figure 6. The cross-coupling TPR peaks are shaded. The heating rate was 2 K/s. (A) The formation of the cross-coupling product, $CF_3(CH_2)_4CH_3$, at 217 K is evident from the fragmentation pattern which has signals at m/e = 140 (parent ion), 121 ($CF_2(CH_2)_4CH_3^+$), and 120 ($CF_2(C_4H_7)CH_3^+$) at a reduced ionizer energy (E_I) of 33 eV. The initial coverages of $CH_3CH_2CH_{2(ad)}$ and $CF_3CH_2CH_{2(ad)}$ were high, i.e. 0.5 and 0.33 ML, respectively. (B) The cross-coupling reaction temperature is 220 K for a high initial coverage of $CH_3CH_2CH_{2(ad)}$ and a low coverage of $CF_3CH_2CH_{2(ad)}$ and was detected for m/e = 69 and 110 fragments at E_I of 70 eV.

In particular, if the cross-coupling reaction temperature were to reflect the kinetic parameters of the reaction, it is important that the coverage of both the reactants be comparable at the cross-coupling temperatures. This was achieved in the TPR experiments in Figure 7B where the Ag(111) surface was exposed to a high initial coverage of $CH_3CH_2CH_{2(ad)}$ (0.75 ML) and a low coverage of $CF_3CH_2CH_{2(ad)}$ (0.2 ML). At these initial coverages, even though a large fraction of $CH_3CH_2CH_{2(ad)}$ self-couples at lower temperature (i.e. at 205 K in Figure 7B), the coverage of $CH_3CH_2CH_{2(ad)}$ left on the surface at the cross-coupling temperature is comparable to the surface coverage of $CF_3CH_2CH_{2(ad)}$. The cross-coupling reaction temperature in Figure 7B is 220 K and it is listed in column 5 of Table 2. The mass spectrometer ionizer energy in Figure 7B was 70 eV, and more intense fragments were monitored in these experiments in order to obtain better signal-to-noise ratios in the TPR spectra.

4. Discussion

The primary aim of this study is to probe the electronic nature of the reaction center during the course of the coupling reaction of alkyl groups on the Ag(111) surface. Accordingly we have divided the discussion into three sections. Section 4.1 discusses the kinetic parameters determined experimentally for the coupling of ethyl groups and propyl groups. Based on these values of ν the kinetic parameters for the coupling reactions of all the other alkyl groups are calculated. These kinetic parameters are utilized to plot linear free energy relationships (LFER) as described in section 4.2. Finally, in section 4.3 the electronic structure of the reaction center during the coupling of alkyl groups is discussed in light of the LFER plots.

4.1. Kinetic Data Analysis. The activation energies for ethyl coupling and propyl coupling reactions are very similar, i.e. E_a = 16.9 ± 0.4 kcal/mol and E_a = 15.1 ± 0.6 kcal/mol, respectively (Figure 3 and section 3.1). These values of E_a are tabulated in column 7 of Table 2. The pseudo-first-order pre-exponential factors are $10^{16.7\pm0.8}$ and $10^{17.1\pm0.4}$ s^{-1}, respectively, and are listed in column 6 of Table 2. These values of pre-exponential factors are significantly greater than 10^{13} s^{-1}. There are a number of possible reasons for this, but the usual transition state argument is that the transition state (TS) is more loosely bound than the initial state.[43] For alkyl coupling a "loose transition state" can be envisioned as a TS capable of free translation on the two-dimensional surface and free rotation parallel to the surface while the initial state is a rigidly bound surface alkyl group. The ratio of the pre-exponential factors for two different alkyl coupling reactions (e.g. A + A and B + B) is then a ratio of the corresponding translational and rotational partition functions of the transition states, i.e. eq 4.1.1,

$$\frac{\nu_{AA}}{\nu_{BB}} = \frac{(q_{rot})^{\ddagger}_{AA}(q_{transl})^{\ddagger}_{AA}}{(q_{rot})^{\ddagger}_{BB}(q_{transl})^{\ddagger}_{BB}} \qquad (4.1.1)$$

where the $q^{\ddagger}$'s are the partition functions of the transition states. Equation 4.1.1 is a general expression for the pre-exponential factors for any alkyl coupling reaction.

Fluorination of the terminal methyl group in adsorbed propyl groups results in an increase of the coupling reaction temperature by ~70 K (column 5, Table 2). A direct experimental evaluation of the kinetic parameters by variable heating rate TPR measurements for the coupling reaction of $CF_3CH_2CH_{2(ad)}$ was unsuccessful as other reactions compete at the same temperature (see section 3.2). A similar situation exists for the cross-coupling reactions of (a) $CH_3CH_{2(ad)}$ + $CF_3CH_2CH_{2(ad)}$, Figure 6, and (b) $CH_3CH_2CH_{2(ad)}$ + $CF_3CH_2CH_{2(ad)}$, Figure 7, where self-coupling reactions are an additional complication. The pre-exponential factors for all these reactions were instead calculated starting from expression 4.1.1 and using ν for the $CH_3CH_2CH_{2(ad)}$ self-coupling reaction (similar results are obtained if ν for the self-coupling of $CH_3CH_{2(ad)}$ is used). Equation 4.1.1 can be simplified further by approximating the rotational motion of the "loose transition state" with a rigid rotor model where the terminal CH_3 and/or CF_3 (or $(CH_3)_2CH$ for isopropyl coupling) groups contribute to the bulk of the mass held rigidly at the ends of the rotor by the intervening $-CH_2-$ groups (or the intervening C−C bond in the cases of methyl coupling and isopropyl coupling). The result is expression 4.1.2.

$$\frac{\nu_{AA}}{\nu_{BB}} = \left(\frac{2\pi M_{AA}kT/h^2}{2\pi M_{BB}kT/h^2}\right)\left(\frac{8\pi\mu_{AA}(r_{AA})^2kT/h^2}{8\pi\mu_{BB}(r_{BB})^2kT/h^2}\right)$$

$$\frac{\nu_{AA}}{\nu_{BB}} = \left(\frac{M_{AA}\mu_{AA}}{M_{BB}\mu_{BB}}\right)\left(\frac{r_{AA}}{r_{BB}}\right)^2 \qquad (4.1.2)$$

where M is the total mass of the terminal groups (A and/or B) held at a distance of r from each other and μ is their reduced mass. The general form of expression 4.1.2 makes it possible to calculate ν for the coupling reactions of any alkyl groups on the Ag(111) surface, i.e. not only these investigated in this work but also those studied in earlier work by X.-L. Zhou, J. M. White, and co-workers.[8-10] Starting from expression 4.1.2 and the experimentally determined value of ν for the propyl coupling

(43) Zhdanov, V. P. *Surf. Sci. Rep.* **1991**, *12*, 183.

reaction, pre-exponential factors for all other alkyl coupling reactions studied to date on the Ag(111) surface were calculated and the results are shown in column 6 of Table 2. In the calculations involving eq 4.1.2 the distance "r" between the terminal CH_3 and/or CF_3 groups is assumed to be the same for $CH_3CH_2CH_{2(ad)} + CH_3CH_2CH_{2(ad)}$, $CF_3CH_2CH_{2(ad)} + CF_3CH_2CH_{2(ad)}$, and $CF_3CH_2CH_{2(ad)} + CH_3CH_2CH_{2(ad)}$ reactions, as the resulting alkanes have the same chain length, i.e. six carbon atoms. Therefore for the above reactions the ratio of the pre-exponential factors is independent of "r".

However, the reactions $CH_3CH_{2(ad)} + CF_3CH_2CH_{2(ad)}$, $CH_{3(ad)} + CH_{3(ad)}$, and $(CH_3)_2CH_{(ad)} + (CH_3)_2CH_{(ad)}$ yield alkane products with chain lengths different than six carbon atoms. The values of "r" for the transition state of these reactions were extrapolated from that of propyl coupling reaction by assuming (a) a tetrahedral angle at all carbon atoms and (b) the upper and lower limits of the new carbon−carbon bond length as the sum of the van der Waal radii and sum of the covalent radii of carbon, respectively.

The activation energies for alkyl coupling reaction are evaluated from ν and the TPR peak temperatures listed in columns 6 and 5 of Table 2 by using the first-order rate expression.[36] These values of activation energies are tabulated in column 7 of Table 2. Except for the coupling reactions of ethyl groups and propyl groups the values of E_a and ν for all other alkyl coupling reactions listed in Table 2 are calculated as described above. For the cross-coupling reactions, it is assumed that the two different alkyl groups intermix freely on the Ag(111) surface so that the corresponding cross-coupling TPR peak temperatures reflect the real value of the cross-coupling kinetic parameters. Also the cross-coupling reactions were studied at coverages close to saturation due to experimental constraints discussed in section 3.3. Here adsorbate−adsorbate interactions are a potential problem. A shift in the self-coupling temperature of $CF_3CH_2CH_{2(ad)}$ with coverage is one such example (see section 3.2). One must therefore exercise caution in attempting to extract and interpret kinetic parameters under these conditions. In this regard, it is reassuring to note that in each case the cross-coupling reaction occurs between the temperatures for the self-coupling reactions of the participating alkyl groups, a trend expected based on the additivity of inductive substituent effects in LFER studies (see section 4.2).[16-18,20-22] Thus we feel that the value of the kinetic parameters obtained from the peak temperature of these cross-coupling reactions at high coverages is only weakly affected by adsorbate−adsorbate interactions, so that their physical significant is maintained. Finally, in column 8 of Table 2, we have evaluated a rate constant for each of the seven coupling reactions using a temperature of 300 K.

4.2. Linear Free Energy Relationships (LFER). The values of ν and E_a for the alkyl coupling reactions evaluated and discussed in section 4.1 are used to plot linear free energy relationships. The classical examples of LFERs are the Hammett and the Taft equations whose general form is represented by eq 4.2.1:[17,20]

$$-(\Delta G_X^{\ddagger} - \Delta G_0^{\ddagger})/RT = \log\left(\frac{k_X}{k_0}\right) = \sigma_X \varrho \qquad (4.2.1)$$

where $\Delta G^{\ddagger}$ is the free energy of activation, k is the rate constant for the reaction, σ_X is the substituent constant for the substituent group X, ϱ is the reaction constant, the subscript X stands for a substituent group X in the reactant, and the subscript 0 is a reference substituent group for which the value of σ_0 is arbitrarily set to zero (e.g. hydrogen in the Hammett equation and a methyl group in the Taft equation).

The value of σ_X is constant for a substituent group X and is a measure of its electron withdrawing or donating capacity. σ_X varies from one substituent group to another but is independent of the reaction under investigation and the distance of the substitution from the reaction center.[44] Thus, for example, the *inductive* substituent constant for an electron withdrawing group such as fluorine is positive, i.e. $(\sigma_i)_F = 0.5$, while for a weakly electron donating group such as methyl it is negative, i.e. $(\sigma_i)_{CH_3} = -0.05$, for any reaction. Reference 21 gives an extensive list of $(\sigma_i)_X$ for a variety of substituent groups. In addition, in cases where the substituent group can directly participate in resonance with the reaction center, other values such as resonance substituent constants, $(\sigma_R)_X$, have to be used.[16,21,45] The choice of the appropriate kind of σ to be used depends on the molecular structure of the reactant(s). For alkyl groups, where all the carbon atoms are sp^3 hybridized, the effect of a substituent group on the reaction center is through a combination of inductive and field effects.[16,17,45,46] The values of $(\sigma_i)_X$ tabulated in column 3 of Table 2 are taken from ref 21 and take into consideration these inductive and field effects.

The reaction constant, ϱ, on the other hand is constant for a given reaction involving a series of different substituent groups (X) and does not depend on the value of σ_X. In LFER studies the evaluation of ϱ for a reaction is of central importance as it provides insight into the electronic structure of the reaction center and aids in the elucidation of the reaction mechanism. The value of ϱ varies from one reaction series to another and its magnitude depends on a number of factors[16-18,20] including (1) the extent of charge development at the reaction center as the reaction proceeds and (2) the distance of substitution from the reaction center. The sign of ϱ signifies the type of charge developed at the reaction center during the course of the reaction. The value of logarithm k for a reaction involving an electron rich transition state increases linearly with increasing electron withdrawing capacity (i.e. σ is increasing) of a substituent group in the reactant, and according to eq 4.2.1 the value of ϱ for such a reaction is positive. The nucleophilic substitution of CH_3O^- to C_6H_5Cl is an example of a reaction involving an electron rich transition state and ϱ is +8.47.[22] For a reaction involving an electron deficient transition state ϱ is negative. One example is the electrophilic substitution of Cl^+ to C_6H_6 in acetic acid medium which has $\varrho = -10.0$.[22] Interestingly, the sign of ϱ for radical reactions is not easily predicted, but it is usually found to be slightly negative. Two examples[22] are $(C_6H_5COO)_2 \rightarrow 2C_6H_5COO^{\bullet}$ where $\varrho = -0.201$ and $C_6H_5CH_3 + Cl^{\bullet} \rightarrow C_6H_5CH_2^{\bullet} + HCl$ where $\varrho = -1.5$.

Table 2 lists all the alkyl coupling reactions in column 1. The appropriate substituent groups for each coupling reaction are listed in column 2 along with the values of $(\sigma_i)_X$ in column 3. These substituent groups were chosen so that within the reactant(s) they are directly bonded to the α-carbon atom, the reaction center of the alkyl coupling reaction. For example, in methyl coupling, the substituent groups is hydrogen and for propyl coupling the substituent group is CH_3CH_2-. It has been observed in a number of reactions involving reactants with multiple substituent groups that, provided that there are no steric interferences, inductive substituent constants are additive.[16-18,20-22] In addition for bimolecular reactions, substituent groups in both reactants are taken into consideration in LFER plots.[19] Accordingly, for each reaction in Table 2, the sum of $(\sigma_i)_X$ for all the substituent groups in both participating alkyl groups, i.e. $\Sigma_j(\sigma_i)_{X_j}$, is tabulated in column 4. For example, in the cross-

(44) Taft, R. W.; Lewis, I. C. *J. Am. Chem. Soc.* **1958**, *80*, 2442.
(45) Charton, M. *Prog. Phys. Org. Chem.* **1981**, *13*, 119.
(46) Reynolds, W. F. *Prog. Phy. Org. Chem.* **1983**, *14*, 165.

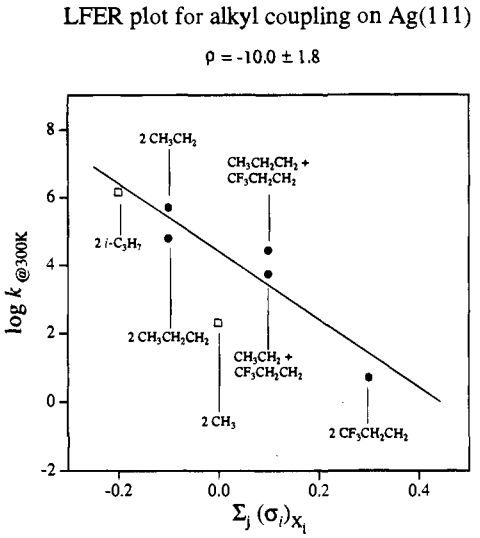

Figure 8. Linear free energy relationship (LFER) for the coupling reaction of alkyl groups on the Ag(111) surface. The values of the inductive substituent constant, $\Sigma_j(\sigma_i)_X$, used are shown in Table 2. Data in solid circles are from the studies in this work and those in hollow squares are from refs 8 and 10. Values of k, the rate constant for each reaction, were evaluated from the kinetic parameters listed in Table 2. The rate of the coupling reaction decreases with the increasing electron withdrawing nature of the substituent group which is reflected in the negative value (i.e. -10.0 ± 1.8) of the reaction constant, ϱ, which is obtained from the slope of the best fit line to the data. The data for CH_3 coupling were not included in this fit.

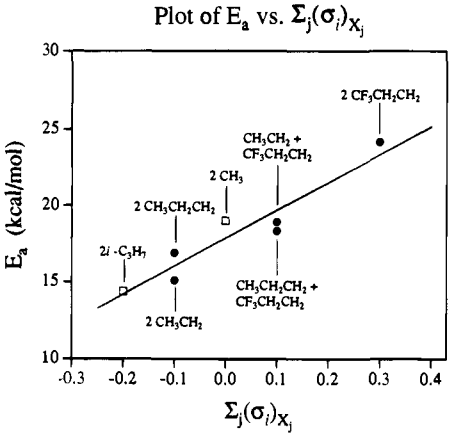

Figure 9. Plot of activation energy (E_a) for the coupling reaction of various substituted alkyl groups as a function of the substituent constants of the substituent group(s), $\Sigma_j(\sigma_i)_X$. The positive slope signifies that the activation barrier to the reaction increases with the electron withdrawing nature of the substituent groups. The implication of this observation is schematically represented in Figure 10.

coupling reaction of $CF_3CH_2CH_{2(ad)} + CH_3CH_2CH_{2(ad)}$ the substituent groups are CF_3CH_2- and CH_3CH_2- so that $\Sigma_j(\sigma_i)_{Xj} = (\sigma_i)_{CF_3CH_2} + (\sigma_i)_{CH_3CH_2} = 0.15 + (-0.05) = 0.1$. Also listed in Table 2 are the TPR peak temperatures (column 5), the values of ν (column 6), and the values of E_a (column 7). The value of log k (log of the rate constant) at 300 K was evaluated for each reaction from the value of ν and E_a using the Arrhenius expression and is tabulated in column 8 of Table 2.

The values of the kinetic parameters and the substituent constants in Table 2 are utilized to obtain the LFER. Figure 8 shows the LFER for alkyl coupling reactions on the Ag(111) surface obtained by plotting log k (at 300 K) against the sum of the *inductive* substituent constants (i.e. $\Sigma_j(\sigma_i)_{Xj}$). Solid circles in Figure 8 are calculated from the results of this study while the hollow squares are those calculated from results of refs 8–10. The results in Figure 8 show that with increasing electron withdrawing nature of a substituent group (i.e. increasingly positive values of σ_i) the alkyl coupling rate decreases. For example, when CF_3 is substituted for CH_3 in both the propyl groups the coupling rate decreases by ~4 orders of magnitude! This negative correlation is also seen from the best line fit to the data shown in the graph of Figure 8. The correlation coefficient is good ($R^2 = 0.94$) when the data for methyl coupling are excluded. The slope of the best fit line is ϱ, the reaction constant, and its value for the coupling of alkyl groups on the Ag(111) surface is -10.0 ± 1.8. Note that a value of $\varrho = -10.5 \pm 1.7$ is obtained if no assumption is made about the loose nature of the transition state and a value of $\nu = 10^{17}$ s^{-1} is used to calculate E_a from the TPR peak temperatures. Thus the general conclusion is not affected by our approximate treatment of a "loosely bound" transition state.

To the best of our knowledge there are no LFER studies of alkyl dimerization reactions in gas- or solution-phase chemistry, thus preventing us from a direct comparison of this surface reaction with reactions in other phases. However, the value of ϱ for alkyl coupling on Ag(111) is higher than the range of ~−6 to +7, typically found for solution-phase reactions.[17,18,20,22] One possible reason is the proximity of the substituent group to the reaction center in the surface coupling of alkyl groups. From the limited number of LFER studies on surfaces it appears that the values of ϱ are generally higher for surface reactions than for solution-phase reactions. Factors such as the lack of solvent effect for reactions on surfaces may be responsible for the high value of reaction constants. Solvents, for example, are well-known to reduce the gas-phase heat of acidity of phenols by as much as a factor of 7![19] In fact the values of ϱ for reactions on surfaces are closer to those observed for gas-phase reactions. For example, ϱ values for formation of olefins from RX on various catalysts are generally within a factor of 0.5 to 2.0 of the values observed for the pyrolytic decomposition of RX to olefin in the gas phase. Another example is the β-hydride elimination reaction of adsorbed alkoxides on copper surfaces, where the value of ϱ is ~0.5 times the gas-phase heat of acidity of the aliphatic carboxylic acids.[25]

The first equality in expression 4.2.1 is valid only if the pre-exponential factors for a reaction involving different substituent groups are the same. The change in a reaction rate due to electronic perturbation by a substituent group is strictly as a result of a change in its activation barrier. Ideally therefore it is more appropriate to plot activation energies against the substituent constants. In most solution-phase and gas-phase reactions, even though it is relatively easy to experimentally determine the rate constant, k, very accurately at 300 K, the individual values of E_a and ν are almost never determined due to the problems associated with temperature-variation measurements. The primary exceptions are the LFERs for acid–base equilibria, where the free energies, obtained from the equilibrium constants, are used.[19] On surfaces a direct measurement of ν and E_a is readily obtained by methods such as those described in section 3.1. Figure 9 shows a plot of E_a vs $\Sigma_j(\sigma_i)_{Xj}$ for the surface coupling reactions of the alkyl groups on the Ag(111) surface. The correlation coefficient for the least-squares fit line to all the data points ($R^2 = 0.96$) is slightly better than that in Figure 8. Note that the data for methyl coupling now correlates well with the rest of the data points and was included in this fit, unlike the line fit in to the data Figure 8. Figure 9 shows that the energy barrier to the alkyl coupling reaction increases with increasing electron withdrawing substitution in the adsorbed alkyl group. This implies that the transition state for this reaction is electron deficient with respect

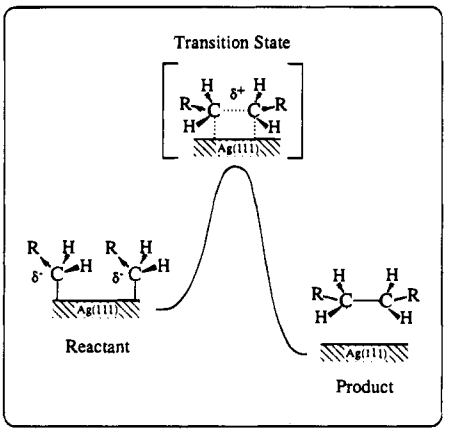

Figure 10. Schematic of the one-dimensional potential energy diagram for the coupling of alkyl groups on a Ag(111) surface. The coupling reaction rate decreases with increasing electron withdrawing nature of the substituent group due to electron deficiency of the transition state with respect to the initial state.

to the initial state. This point is elaborated further in the discussion below.

4.3. Transition State for Alkyl Coupling Reactions. The linear free energy relationship depicted in Figure 9 shows that the activation barrier for alkyl coupling reactions on the Ag(111) surface increases with increasing electron withdrawing nature of the substituent group(s). Since fluorine exerts strong electron withdrawing inductive effects,[23] the results in Figure 9 suggest that the transition state in this reaction is electron deficient compared to the initial state. A schematic representation of the one-dimensional potential diagram for the coupling reaction is shown in Figure 10. The coupling reaction starts with an adsorbed alkyl group as the initial state and passes through a symmetric transition state. The transition state is shown with a partial positive charge and the initial state with a partial negative charge. It is important to point out that from LFER s one can only determine the relative charge separation in the initial and the transition states. One does not know from these studies the absolute charge formation in either state. Thus the charge formation shown in Figure 10 is relative rather than absolute. When hydrogen is substituted with fluorine, the transition state is destabilized and/or the initial state is stabilized leading to a net increase in the reaction activation barrier and hence a decrease in reaction rate.

Although Figure 10 depicts the transition state as symmetric, it is important to note that this may not be the case. It is also important to try to understand why the transition state might be electron deficient with respect to the initial state. There is no easy way to probe the transition state directly. On the other hand, it is relatively easy to probe the initial state, the adsorbed alkyl group. The adsorbed alkyl group may not be neutral. Extended Hückel band calculations by Zheng, Hoffmann, et al. have shown that on transition metal surfaces adsorbed methyl groups have a formal charge between -0.6 and -0.8.[47] Experimental evidence comes from vibrational studies of adsorbed alkyl groups on copper,[48] nickel,[49] and platinum[50] surfaces, where ν_{C-H} mode softening by as much as 180 cm^{-1} was observed. Further, deuterium isotope labeling studies of ethyl groups on copper show that only the α C−H bond undergoes this mode softening.[48] The origin of mode softening has been a subject of debate, but one explanation is that there is an electron transfer from the filled d-orbital of the metal to the σ^*_{C-H} antibonding orbital in the adsorbed alkyl groups.[47,51,52] This charge transfer would not only result in a decrease of the bond order of the α C−H bond leading to the vibrational mode softening but would also impart a formal negative charge to the adsorbed alkyl groups. The transition state for alkyl coupling is then electron poor. Consistent with this explanation are the observations for phenyl coupling. Adsorbed phenyl groups lack σ^*_{C-H} antiboding orbitals at the α-carbon (and therefore cannot participate in the metal d-orbital to σ^*_{C-H} orbital electron transfer process) and have been recently found to couple on copper surfaces at rates which exhibit a positive value of ρ (opposite to that for alkyl coupling).[33]

5. Conclusion

Temperature programmed reaction studies of alkyl groups on the Ag(111) surface show that the alkyl coupling reaction rate decreases with increasing fluorine substitution in the adsorbed alkyl group(s). This observation is consistent with a charge development at the reaction center such that the transition state is electron deficient with respect to the initial state. The electronegative fluorine destabilizes the transition state and/or stabilizes the electron rich initial state.

Acknowledgment. This work was supported by the National Science Foundation under Grant No. CHE-9401276 and Nato Grant No. CRG 930652. A.J.G. holds a Fellowship in Science and Engineering from the David and Lucile Packard Foundation. We thank Jerry M. Meyers for recording the mass spectrum of $CF_3CH_2{=}CH_3$.

JA942905G

(47) Zheng, C.; Apeloig, Y.; Hoffmann, R. *J. Am. Chem. Soc.* **1988**, *110*, 749.
(48) Lin, J.-L.; Bent, B. E. *Chem. Phys. Lett.* **1992**, *194*, 208.
(49) Ceyer, S. T. *Annu. Rev. Phys. Chem.* **1988**, *39*, 479.
(50) Henderson. M. A.; Mitchell, G. E.; White, J. M. *Surf. Sci.* **1987**, *184*, L325.
(51) Schüle, J.; Siegbahn, P.; Wahlgren, U. *J. Chem. Phys.* **1988**, *89*, 6982.
(52) Shustorovich, E.; Baetzold, R. C.; Muetterties, E. L. *J. Phys. Chem.* **1983**, *87*, 1100.